substance: boron compounds with group III elements
property: properties of boron-yttrium and Ln_3MB_7 compounds (except YB_{66})

YB_2

Preparation [75S], crystalline structure [75S]

Entropy in [86B2].

$YCrB_4$

Space group: Pbam

Mentioned in [91D]

Ternary borides containing a rare earth and aluminum, with $YCrB_4$ and Y_2ReB_6 structures [80M]: $YbAlB_4$, $LuAlB_4$ with $YCrB_4$ structure; Yb_2AlB_6 with Y_2ReB_6 type structure.

$Y_3Co_{11}B_4$

Structure ($R_{n+1}\,Co_{3n+5}\,B_{2n}$ type with R = rare earth or Y, n = 2) and electrical resistivity in [96K].

$Y(Rh_{1-x}Ru_x)_4B_4$

Boron local density of states in $Y(Rh_{1-x}Ru_x)_4B_4$ superconductors [83H].

The influence of the formal electric charge on the size of the transition metal atom cluster in YRh_4B_4 and $YRuB_4$ (compared with $PbMo_6S_8$) in [80Y].

$YRuB_2$

Comparative critical field study of superconducting ternary borides [87L].

RE_3MB_7

Space group: Cmcm

The borides R_3ReB_7 (R = Gd, Tb, Dy, Ho, Er, Tm), R_3FeB_7 (R = Y, Tb, Dy, Ho, Er) and R_3MnB_7 (R = Y, Gd) are isotypic with Er_3CrB_7.

Projection of the crystal structure of Er_3CrB_7 along the *x* axis in Fig. 1 [86K].

lattice parameters

Compound	*a* (in nm)	*b* (in nm)	*c* (in nm)	*V* (in nm^3)	
Y_3MnB_7	0.3464(1)	1.5696(1)	0.9313(1)	0.506	86K
Gd_3MnB_7	0.3488(1)	1.5875(1)	0.9399(1)	0.520	
Y_3ReB_7	0.3537(2)	1.5848(8)	0.9396(5)	0.527	
Gd_3ReB_7	0.3576(2)	1.60264	0.9462(2)	0.542	
Tb_3ReB_7	0.3544(1)	1.5884(3)	0.9400(2)	0.529	
Dy_3ReB_7	0.3557(2)	1.5789(5)	0.9359(3)	0.526	
Ho_3ReB_7	0.3515(2)	1.5743(5)	0.9360(3)	0.518	
Er_3ReB_7	0.3501(1)	1.5691(3)	0.9346(1)	0.513	
Tm_3ReB_7	0.34744	1.5582(7)	0.9307(3)	0.504	
Y_3FeB_7	0.3423(1)	1.5658(6)	0.9295(5)	0.498	
Tb_3FeB_7	0.3974(2)	1.56404	0.9413(2)	0.500	
Dy_3FeB_7	0.3375(2)	1.5540(6)	0.9403(3)	0.493	
Ho_3FeB_7	0.3369(1)	1.5504(5)	0.9358(2)	0.489	
Er_3FeB_7	0.3363(2)	1.5341(5)	0.9350(2)	0.482	

Variation of the unit cell size of Er_3CrB_7 type structures depending on the atomic number of the rare earth metal in Fig. 2 [86K].

$YREB_6$

Mentioned in [91D].

YB_4

preparation [75S], crystalline structure [63R], electrical and thermal conductivity [74S]

Semimetal [84T].

Crystal structure in Fig. 3 [85T], see also [84T].

Brillouin zone in Fig. 4 [85T].

Preparation of single crystals in [84T].

electronic properties

Schematic diagram of the electronic structure of YB_4 assumed to result as a superposition of those of YB_6 and YB_2 in Fig. 5 [85T].

Anisotropy of the de Haas-van Alphen frequencies in Fig. 6 [84T, 85T].

Fermi surface determination by use of the de Haas-van Alphen effect in [85T].

melting point

T_m	2800 °C			96G

entropy

Entropy in [86B2].

microhardness

H_K	2200...2880 kg mm^{-2}	T = 300 K	load 50 g	96G

YRh_4B_4

critical temperature of superconductivity

T_c	11.34 K			91F, 77M2

Superconductivity in the pseudoternary system YRh_4B_4-$LaRh_4B_4$-$ThRh_4B_4$ [81H].

YB_6

superconducting, semimetal?; preparation [75S, 76F, 77P], crystalline structure [75S, 76F], magnetic susceptibility [79S], electrical conductivity [76F], electronic transport properties [71G], ESCA spectrum [76A].

Calculated total electronic density of states in Fig. 7 [82S].

The Eliashberg function and the superconducting T_c in [80S].

critical temperature of superconductivity

T_c	5.7 K			91F, 68M
	8.4			76F 69F

Phonon density of states calculation in Fig. 8 [82S].

Electron tunneling [84K, 87S], second derivative of the tunnel current in Fig. 9.

Raman spectrum of amorphous YB_6 ($YB_{8.5}$) in Fig. 10 [80L].

microhardness

H_K	2690 kg mm^{-2}	T = 300 K	cube, average value, load 20 g	96G

melting point

T_m	2600 °C		melting with decomposition	96G

Thermal expansion coefficient: α [10^{-6}K^{-1}] = 4.0097 (1+5.82·10^{-6} T + 2.36·10^{-9} T^2), T in K [73D].

Entropy in [86B2].

YB_{12}

preparation [65M1, 75S, 65M2], crystalline structure [65M1, 65M2, 77M1, 60B1], magnetic susceptibility [79M, 73O]

Density of states calculation in Fig. 11 [86S]; valence band density of states in [86B1], for component density of states [86S].

critical temperature of superconductivity

T_c	4.7 K		possibly due to the second phase YB_6	91F 68M

entropy

S	109(123) J K^{-1} mol^{-1}			86B2

$YAlB_{14}$

On preparation and crystal habit see [94D].

lattice parameters
(in Å)

a	5.8212(3)	T = 300 K	$Y_{0.62}Al_{0.71}B_{14}$, X-ray diffraction	93W, 92K
b	8.1947(6)			
c	10.4130(8)			

site occupancies

Y	0.310(1)	T = 300 K	$Y_{0.62}Al_{0.71}B_{14}$	92K
Al	0.708(3)			
B(1) – B(5)	1.0			

atomic distances
(in Å)

d	2.27		Al – 12B	93W
	2.71		Y – 16B	
	2.91		Al – Al	
	3.16/3.11/3.66		Li – Li	

microhardness
(for load p = 100 g, in kg mm^{-2})

H_K	3700 / 3300	T = 300 K	(001) for azimuth 45 / 90°	94D
	3400 / 2600		(011) for azimuth 0 / 45°	

YB_{25}

Structure

Structure: monoclinic

Space group: I121, I1m1, I12/m1 [97T1].

Single phase YB_{25} is obtained at mixing ratios of n = 25.5 and 26.0 [97T1].

lattice parameters
(in nm)

a	0.82842(3)	T = 300 K	X-ray powder diffraction and	97T1
b	1.03203(3)		electron diffraction	
c	0.58570(2)			
β	90.402(3)°			
V	0.50073(3) nm^3			

YB_{50}

Structural type similar to γ-AlB_{12}

Space group: $P2_12_12_1$ [97T2].

(Previous structure characterization: orthorhombic structure, space group $P2_12_12$ [94T].)

Preparation in [94T].

lattice parameters
(in nm)

a	1.66251(9)	T = 300 K	powder X-ray diffraction	94T
b	1.76198(11)			
c	0.94797(3)			
V	2.7768(3) nm^3			

$YB_{44}Si_{1.0}$

Structure: orthorhombic

Space group: Pbam or Pba2 [97T2].

Single crystal growth (compositions between $YB_{41.5}Si_{2.82}$ and $YB_{44.4}Si_{1.04}$) in [97T2].

$YB_{41}Si_{1.2}$

The unit cell contains five crystallographically different B_{12} icosahedra. A peculiarity of the structure are $B_{12}Si_3$ polyhedral units aside from five crystallographically different B_{12} icosahedra [97H] (Figs. 12...15 [97H]).

Structure: orthorhombic

Space group: Pbam

lattice parameters
(in Å)

a	16.674(1)	*T* = 300 K	single crystal X-ray diffractometry	97H
b	17.667(1)			
c	9.5110(7)			

occupancies

The occupancies of the B sites in the five B_{12} icosahedra are 1.0, each [97H].

occupancies of sites in the $B_{12}Si_3$ structural units (B(Si)n and B(Si)n) and single atomic sites

Atom	Site	*x*	*y*	*z*	Occupancy	
B6.1 –B6.6	8(i)				1.0	97H
Si6.7	4(h)	02784(3)	0.3866(3)	½	0.575(6)	
B6.7	4(h)	0.2785(13)	0.3961(11)	½	0.425(6)	
Si6.8	4(h)	0.4429(3)	0.2787(2)	½	0.478(6)	
B6.8	4(h)	0.4492(11)	0.2818(12)	½	0.522(6)	
Si6.9	4(h)	0.4655(3)	0.4626(3)	½	0.440(6)	
B6.9	4(h)	0.4589(9)	0.4537(7)	½	0.560(6)	
B7.1	8(i)	0.3911(4)	0.3747(4)	0.1181(8)	1.0	
B7.2	8(i)	0.3182(17)	0.2183(16)	0.502(31)	0.46(1)	
B7.3	4(g)	0.4569(3)	0.0212(2)	0	0.23(1)	
B7.4	4(g)	0.0766(4)	0.1555(6)	0	0.29(1)	
B7.5	4(g)	0.1438(11)	0.2507(11)	0	0.18(1)	
B7.6	4(g)	0.2552(10)	0.2629(9)	0	0.43(1)	
B7.7	4(h)	0.2054(15)	0.0230(14)	½	0.08(1)	
Y	8(i)	0.29628(1)	0.05199(1)	0.22964(3)	1.0	
Si	8(h)	40.3440(2)	0.07974(8)	½	0.798(6)	

Physical properties

resistivity

ρ	0.l5 Ω cm	*T* = 300 K	$T^{-1/4}$ dependence	99I

Hall mobility

μ_H	~0.l $cm^2V^{-1}s^{-1}$	*T* = 300 K	99I

thermoelectric power

S	180 μV K^{-1}	*T* = 110...290 K	decrease towards lower *T*	99I

References:

60B1 Binder, I., La Placa, S., Post, B., in: Boron I, J. A. Kohn, W. F. Nye, G. K. Gauld, eds., Plenum Press: New York, 1960 p. 86.

60B2 Becher, H.J.: Z. Anorg. Allg. Chem. 306 (1960) 266.

60K Kohn, J. A.: see [60B1], p. 75.

63R Rudman, R., La Placa, S., Post, B.: Acta Crystallogr. 16 (1963) 29.

65M1 Matkovich, V. I., Giese, R. F., Economy, J.: Z. Kristallogr. 122 (1965) 116.

65M2 Matkovich, V. I., Economy, J., Giese, R. F., Barret, R.: Acta Crystallogr. 19 (1965) 1056.

68M Matthias, B.T., Geballe, T.H., Andres, K., Corenzwit, E., Hull, W., Maita, J.P.: Science 159 (1968) 530.

69F Fisk, Z., Matthias, B.T., Corenzwit, E.: Proc. Nat. Acad. Sci. 64 (1969) 1151.

71G Gorjachev, Yu. M., Odintsov, V. V., Paderno, Yu. B.: Metallofizika, Kiev (USSR) 37 (1971) 29.

73D Dudchak, Ya.I., Fedishin, Ya.I., Paderno, Yu.B., Vadez, D.I.: Izv. Akad. Nauk. SSSR Ser. Fiz. 1 (1973) 154 (in Russian).

73O Odintsov, V. V., Kostetskii, I. I., L'vov, S. N.: Izv. Akad. Nauk, Neorg. Mater. 9 (1973) 944: (engl. Transl. in Inorganic materials).

74S Severyanina, F. N., Dudnik, E. M., Paderno, Yu. B.: Poroshk. Metall. 13 (1974) 83.

75S Samsonov, G. V., Serebryakova, T. I., Neronov, V. A.: Boridy, Moskva Atomizdat, 1975.

76A Aono, M., Kawai, S., Kono, S., Okusawa, M., Sagawa, T., Takehana, Y.: J. Phys. Chem. Solids37 (1976) 215.

76F Fisk, Z., Schmidt, P. H., Longinotti, L. D.: Mater. Res. Bull. 11 (1976) 1019.

77B Berezin, A. A., Golikova, O. A., Zaitsev, V. R., Kazanin, M. M., Orlov, V. M., Tkalenko, E. N., in:Boron and Refractory Borides, (Matkovich V. 1., ed.) Springer: Berlin, Heidelberg, New York 1977, p. 52.

77M1 Matkovich, V. I., Economy, J.: see [77B], p. 78.

77M2 Matthias, B.T., Corenzwit, E., Vandenberg, J.M., Barz, H.: Proc. Nat. Acad. Sci. 741 (1977) 1334.

77P Pastor, H.: see [77B], p. 457.

79M Moiseenko, L. L., Odintsov, V. V.:J. Less-Common Met. 67 (1979) 237.

79S Sobezak, R. J., Sienko, M. J.: J. Less-Common Met. 67 (1979) 167.

80L Lannin, J.S., Messier, R.: Phys. Rev. Lett. 45 (1980) 1119.

80M Mikhalenko, S.I., Kuz'ma, Yu.B., Korsukova, M.M., Gurin, V.N.: Inorg. Mater. 16 (1980) 1325.

80S Schell, G., Winter, H., Rietschel, H.: in: Superconductivity in d- and f-band metals. Proc. Conf. Supercond. In d- and f-band metals, H. Suhl, M.B. Maple ed., Academic: London, 1980, p. 465.

80Y Yvon, K., Gruttner, A.: in: Superconductivity in d- and f-band metals. Proc. Conf. Supercond. in d- and f-band metals, H. Suhl, M.B. Maple ed., Academic: London, 1980, p. 515.

81H Hiebl, K., Rogl, P., Sienko, M.J.: J. Less-Common Met. 82 (1981) 201.

82S Schell, G., Winter, H., Rietschel, H., Gompf, F.: Phys. Rev. B 25 (1982) 1589.

83H Hamaker, H.C., Zajac, G., Bader, S.D.: Phys. Rev . B 27 (1983) 6713.

84K Kunii, S., Kasuya, T., Kadowaki, K., Date, M., Woods, S.B.: Solid State Commun. 52 (1984) 659.

84T Tanaka, T., Otani, S., Ishizawa, Y.: J. Less-Common Met. 102 (1984) 281.

85T Tanaka, T., Ishizawa, Y.: J. Phys. C: Solid State Phys. 18 (1985) 4933.

86B1 Bullett, D.W.: in: Boron-Rich Solids (AIP Conf. Proc. 140), Albuquerque, New Mexico 1985, D. Emin, T.L. Aselage, C.L. Beckel, I.A. Howard ed., American Institute of Physics: New York, 1986, p. 249.

86B2 Borovikova, M.S., Fesenko, V.V.: J. Less-Common Met. 117 (1986) 287. (Proc. 8th Int. Symp. Boron, Borides, Carbides, Nitrides and Rel. Compounds, Tbilisi, Oct. 8 - 12, 1984)

86K Kuz'ma, Yu.B., Mykhalenko, S.I., Akselrud, L.G.: J. Less-Common Met. 117 (1986) 29 (Proc. 8th Int. Symp. Boron, Borides, Carbides, Nitrides and Rel. Compounds, Tbilisi, Oct. 8 - 12, 1984).

86S Switendick, A.C.: in: Boron-Rich Solids (AIP Conf. Proc. 140), Albuquerque, New Mexico 1985, D. Emin, T.L. Aselage, C.L. Beckel, I.A. Howard ed., American Institute of Physics: New York, 1986, p. 260.

87L Lee, W.H., Shelton, R.N.: J. Low Temp. Phys. 68 (1987) 147.

87S Schneider, R., Geerk, J., Rietschel, H.: Europhys. Lett. 4 (1987) 845.

91D Derkhachenko, L.I., Gurin, V.N., Korsukova, M.M., Nechitailov, A.A., Nechitailov, A.P., Kuz'ma, Yu.B., Chaban, N.F.: in: Boron-Rich Solids, Proc. 10th Int. Symp. Boron, Borides and Rel. Compounds, Albuquerque, NM 1990 (AIP Conf. Proc. 231), D. Emin, T.L. Aselage, A.C. Switendick, B. Morosin, C.L. Beckel ed., American Institute of Physics: New York, 1991, p. 451.

91F Fisk, Z.: in: Boron-Rich Solids, Proc. 10th Int. Symp. Boron, Borides and Rel. Compounds, Albuquerque, NM 1990 (AIP Conf. Proc. 231), D. Emin, T.L. Aselage, A.C. Switendick, B. Morosin, C.L. Beckel ed., American Institute of Physics: New York, 1991, p. 155.

92K Korsukova, M.M., Lundström, T., Tergenius, L.-E., Gurin, V.N.: J. Alloys Compounds 187 (1992) 39.
93W Werheit, H., Kuhlmann, U., Krach, G., Higashi, I., Lundström, T., Yu, Y.: J. Alloys Compounds 202 (1993) 269.
94D Derkachenko, L., Gurin, V., Korsukova, M., Nechitailov, Alexei, Nechitailov, Andrei: Proc. 11th Int. Symp. Boron, Borides and Rel. Compounds, Tsukuba, Japan, August 22 - 26, 1993, Jpn. J. Appl. Phys. Series 10 (1994), p. 144.
94T Tanaka, T., Okada, S., Ishizawa, Y.: J. Alloys Compounds 205 (1994) 281.
96G Gurin, V.N., Derkachenko, L.I., Korsukova, M.M., Nikanorov, S.P., Jung, W., Müller, R.: Sov. Phys. Solid State 38 (1996) 1508.
96K Kowalczyk, A., Ivanov, V.: Phys. Status Solidi 193 (1996) 155.
97H Higashi, I., Tanaka, T., Kobayashi, K., Ishizawa, Y., Takami, M.: J. Solid State Chem. 133 (1997) 11 (Proc. 12th Int. Symp. Boron, Borides and Rel. Compounds, Baden, Austria, 1996).
97T1 Tanaka, T., Okada, S., Yu, Y., Ishizawa, Y.: J. Solid State Chem. 133 (1997) 122 (Proc. 12th Int. Symp. Boron, Borides and Rel. Compounds, Baden, Austria, 1996).
97T2 Tanaka, T., Okada, S., Ishizawa, Y.: J. Solid State Chem. 133 (1997) 55 (Proc. 12th Int. Symp. Boron, Borides and Rel. Compounds, Baden, Austria, 1996).
99I Ishizawa, Y., Tanaka, T.: J. Solid State Chem. (2000) (Proc. 13th Int. Symp. Boron, Borides and Rel. Compounds, Dinard, France, Sept. 1999).

Fig. 1.

Er_3CrB_7. Projection of the crystal structure along the *x* axis. Stacking of trigonal prisms of metal atoms is shown by continuous lines; broken lines indicate the connection of boron atoms [86K].

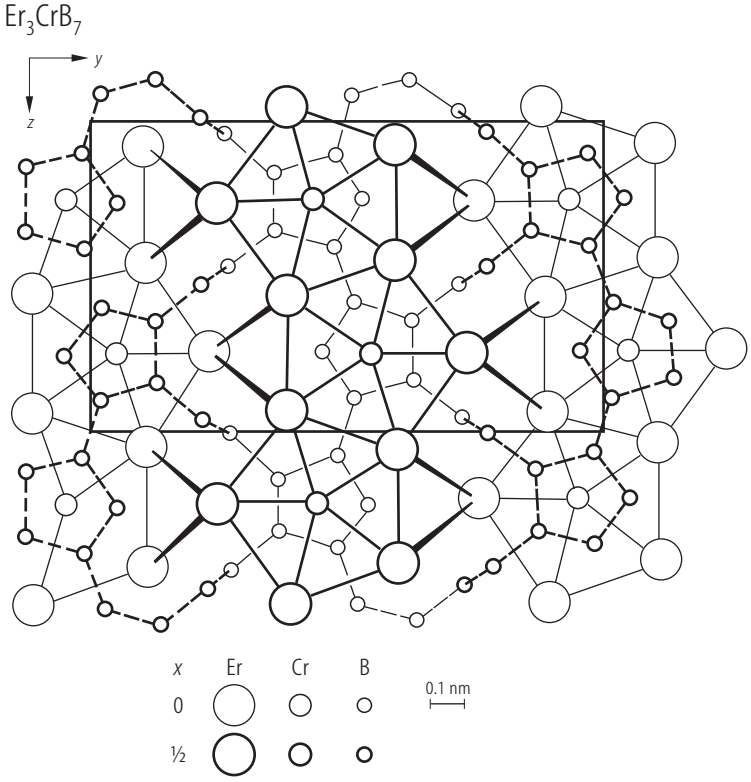

Fig. 2.

Er_3CrB_7 type. Variation of the unit cell size depending on the atomic number of the rare earth metal (Gd, 64 – Er, 68) [86K].

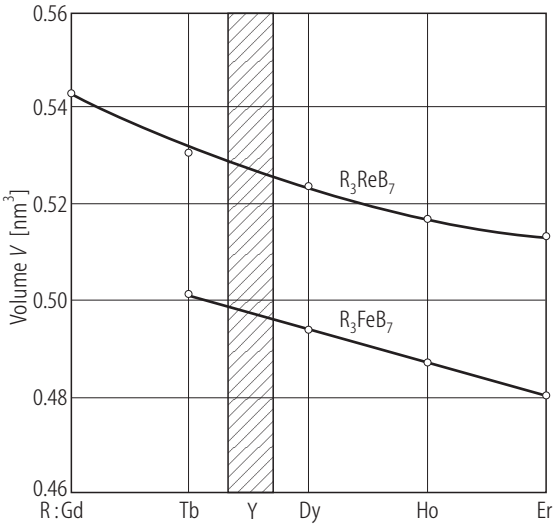

Fig. 3.

YB_4. Crystal structure. Large circles, metal atoms; small circles, boron atoms. The planes indicated by dashed lines denote metal and boron layers [85T].

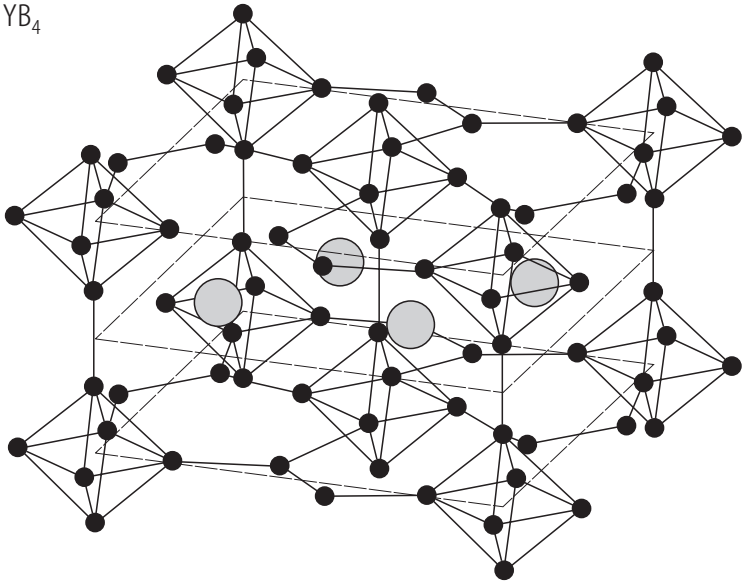

Fig. 4.

YB_4. Brillouin zone [85T].

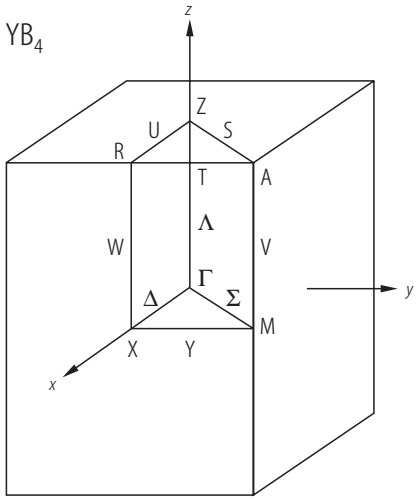

Fig. 5.

YB_4. Schematic diagram of the electronic structure of YB_4 assumed to result as a superposition of those of YB_6 and YB_2 [85T].

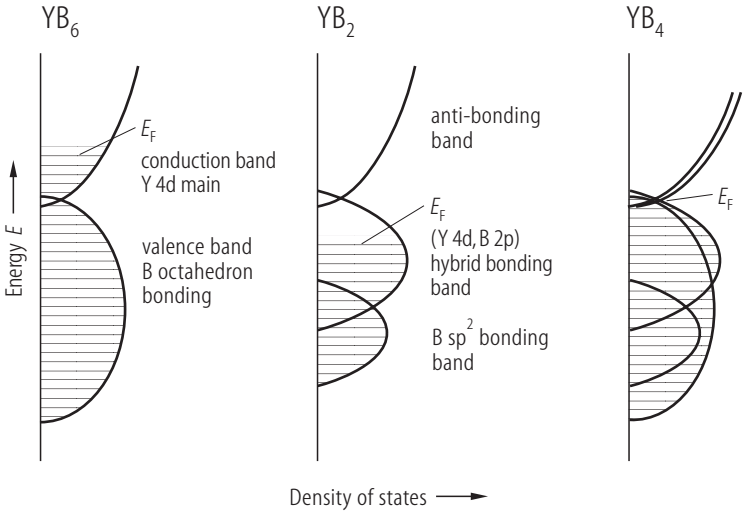

Fig. 6.

YB_4. Anisotropy of the de Haas-van Alphen frequencies for three principal planes [84T, 85T].

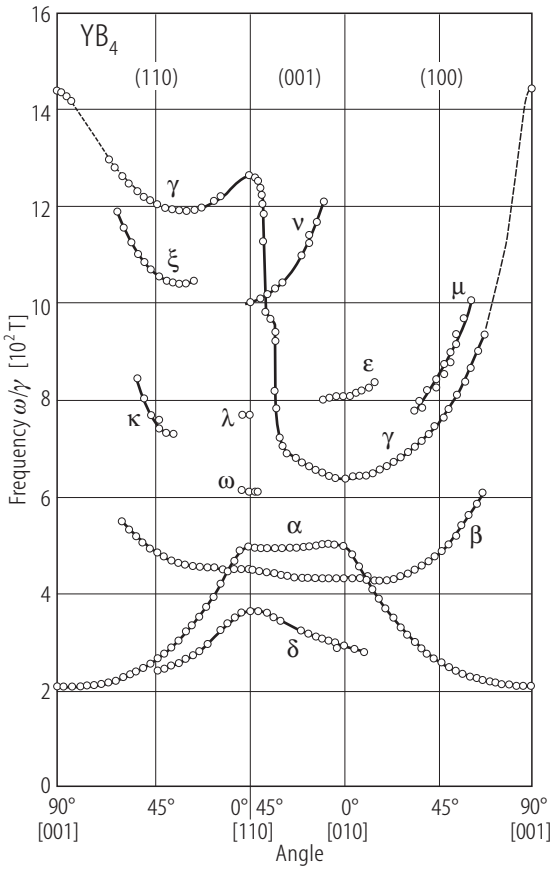

Fig. 7.

YB_6. Calculated total electronic density of states [82S].

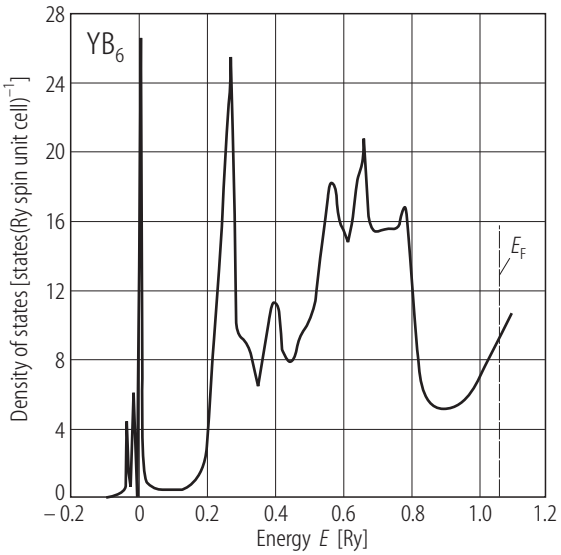

Fig. 8.

YB_6. Calculated phonon density of states [82S].

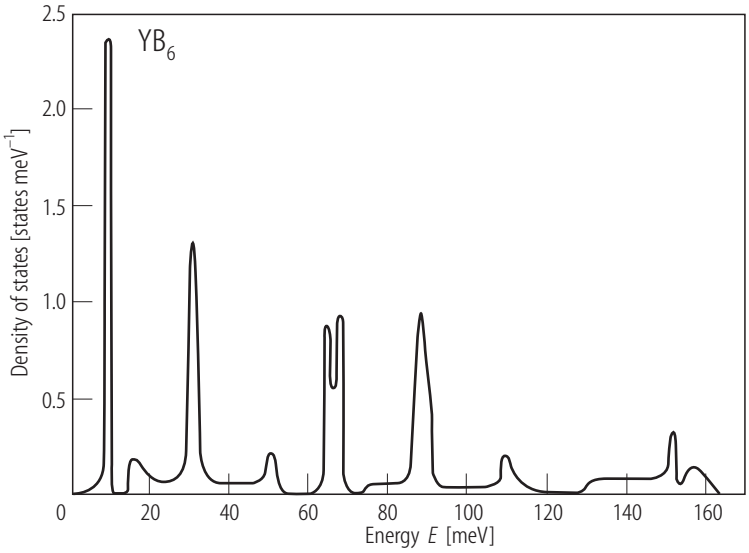

Fig. 9.

YB_6. Second derivative ($-d^2I/dV^2$ vs. voltage V for a YB_6/YB_6-oxide/In tunnel junction with YB_6 in the superconducting (solid line) (T = 1.2K) and normal conducting (dashed line) (T = 8 K) state. The In counterelectrode is normal conducting [87S]. Dotted line (upper part), second derivative measurement using a GaAs point contact method [84K].

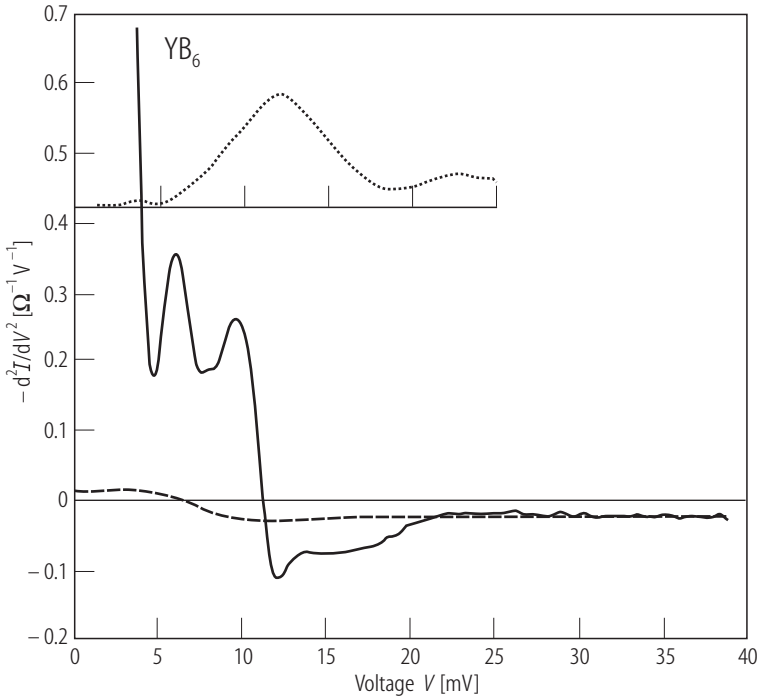

Fig. 10.

a-$YB_{8.5}$. Raman spectrum; Raman intensity vs. wavenumber. The arrow indicates an approximate peak in the density of states for c-YB_6 obtained by neutron scattering [80L].

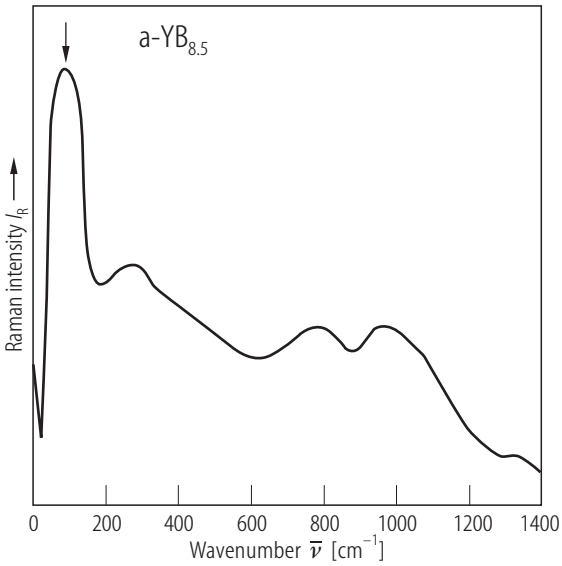

Fig. 11.

YB_{12}. Calculated total electronic density of states [86S].

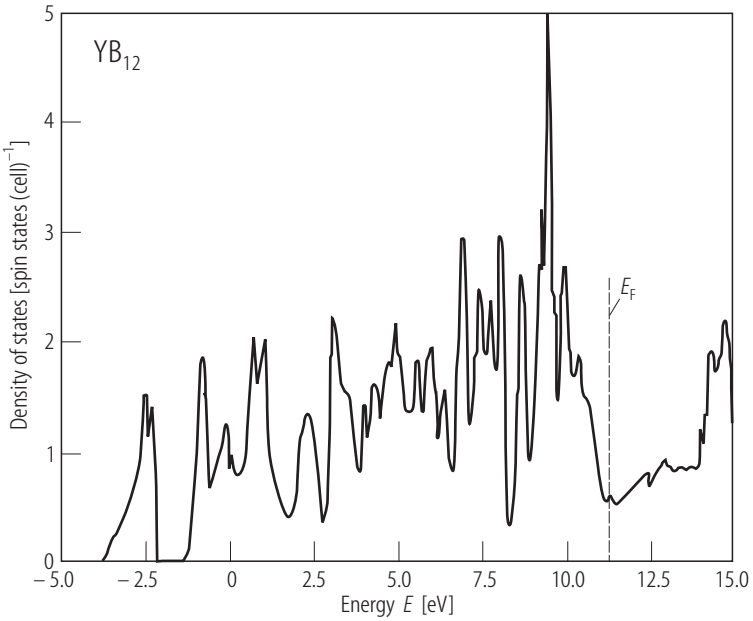

Fig. 12.

$YB_{41}Si_{1.2}$. Icosahedral B_{12} arrangement as seen along the *c* axis (only the icosahedra within the range *z* = 0.17...0.42 are drawn) [97H].

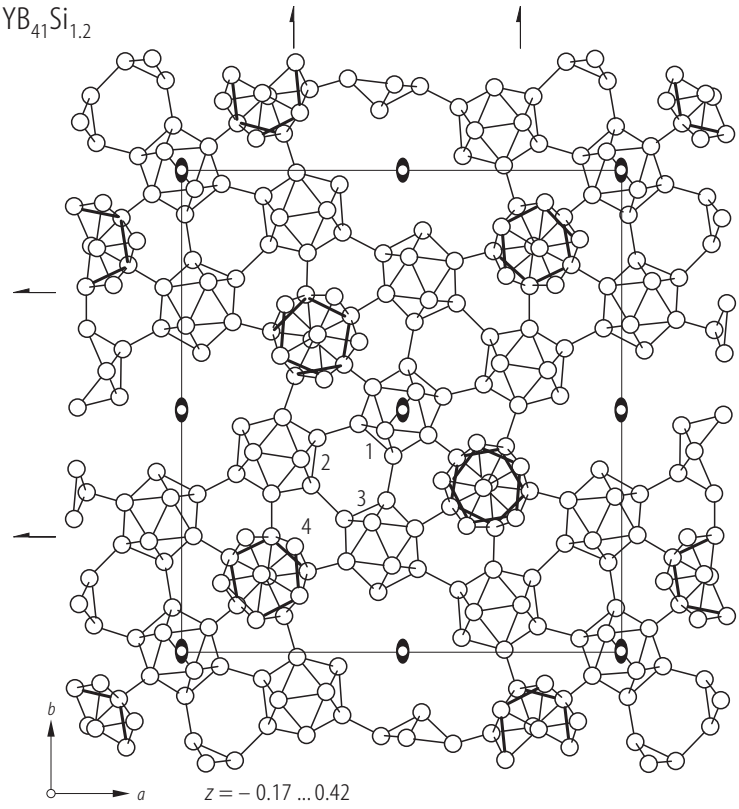

Fig. 13.

$YB_{41}Si_{1.2}$.Arrangement of B_{12} icosahedra and $B_{12}Si_3$ units as seen along the *c* axis. Polyhedra within the range *z* = 0.30...0.92 are drawn [97H].

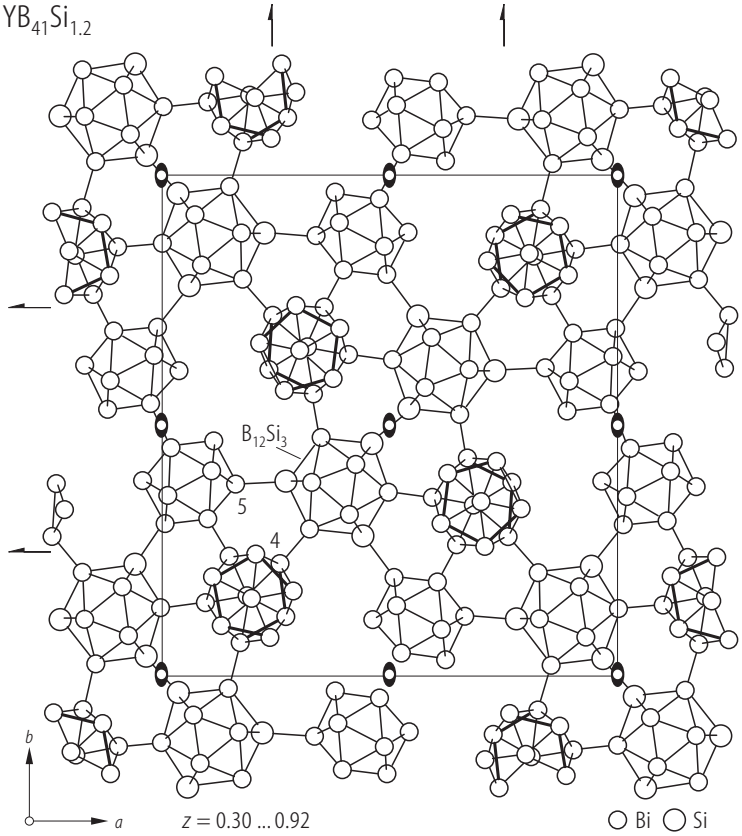

Fig. 14.

$YB_{41}Si_{1.2}$. $B_{12}Si_3$ unit as seen along the *b* axis. Large circles, Si sites; smaller circles, B sites [97H].

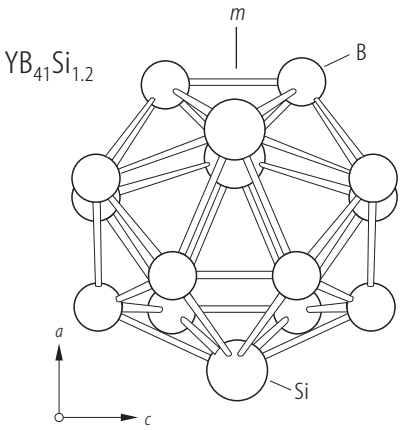

Fig. 15.

$YB_{41}Si_{1.2}$. Unusual linkage between two icosahedra effected through two apical atoms of each icosahedron [97H].